

**Synthesis of sulfide Nano composites using Na-4 mica template****Joyshree Maji^{*1}, Soumen Basu² and Pijus kanti.Mukherjee³**

1. Dept. of Physics, Asansol Engineering College, Asansol, West Bengal, **INDIA**
2. Dept. of Physics, National Institute of Technology, Durgapur, West Bengal, **INDIA**
3. Dept. of Physics, Durgapur Govt. College, West Bengal, **INDIA**.

Email: joyshreephy@yahoo.com, Soumen_basu@yahoo.comReceived on 24th June and finalized on 3rd July 2013.**ABSTRACT**

Various Nano composites were synthesized using mica crystallites medium. In some cases by oxidation or sulfidation treatment a core shell nanostructure could be generated. Nickel sulfide core shell Nano rod exhibited a number of optical absorption peaks which arose because of their structural characteristics. Nickel sulfide nano wire of diameter, 20 nm, were grown within nano channels of Na-4 mica.

Keywords: Sol-gel process, Nano composites, Electrical Properties, Al₂O₃.**INTRODUCTION**

Nano composites are materials in which a phase with nanoscale dimensions is dispersed within a matrix. These matrixes have acquired significance because of interesting physical properties exhibited by them. Various techniques have been used to synthesize these materials. We have synthesized NiS nano composites using mica structure as medium. By suitable oxidation of the composite a core shell nanostructure was developed in them. Materials exhibited interesting electrical and optical properties.

MATERIALS AND METHODS

The channels within a high charge density sodium fluorphlogopite mica channels of chemical composition, Na₄Mg₆Al₄Si₄O₂₆F₄, xH₂O (Kodama and Komarneni 1999) were used to grow NiS nanowires of diameter (1.3nm). Mica of the above mentioned composition is commonly referred to as Na-4 Mica. This was prepared by a sol gel method. The chemicals used were Al (NO₃).9H₂O, Mg (NO₃)₂.6H₂O and Si (OC₂H₅)₄. The latter were dissolved in C₂H₅OH and the solution was stirred for 3hr. The amounts of the compounds were chosen such that the final composition would be MgO.Al₂O₃.2SiO₂. The gel was dried at 373K calcination done at 748K for 10hr. The gel powder was mixed thoroughly with an equal amount of NaF powder. The treatment at 1163K for 16 hr in a platinum crucible. After washing the reaction products with deionized water and then with saturated boric acid. They were washed with 1M NaCl to saturate all exchange sites with Na⁺. After subsequent washing with deionized water. Solid was dried at 333K for 3 days. 2 gm of Na-4 mica powder was then immersed into 25cc of 0.4(M) Ni (SO₄) to which 0.5 (M) NaCl solutions was added. This brought about an ion exchange reaction of the type Ni⁺² to 2Na⁺ which

continued for a period of 4 weeks at 303K. After separating the ion exchanged powder from the solution by a centrifuge, it was subjected to a heat treatment in H₂S at 673K for 1hr. This produced NiS wires within the Na-4 mica channels.

RESULTS AND DISCUSSION

Corresponding to the shell reaction feature identified powder X ray diffraction (XRD) of this sample revealed the presence of two crystal structures: one is tetragonal and the other is monoclinic. The vertical lines indicate the positions and intensities of XRD peaks of powder NiS. The figure shows the corresponding XRD patterns at higher resolution. All salient diffraction peaks can be closely matched to the monoclinic and tetragonal structures. Among these two structural phases, the monoclinic phase appears to be more abundant based on the XRD data.

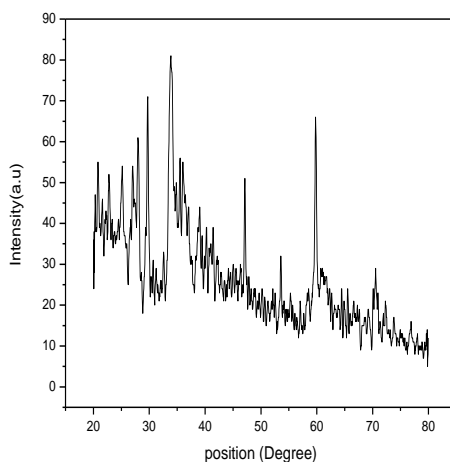


Figure 1. X.R.D Graph

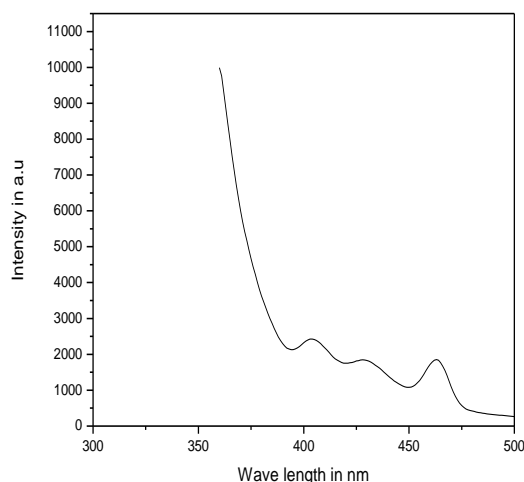


Figure 2. Graph for Photo Luminescence

Above fig shows the PL spectrum from the as synthesized NiS nanoparticles (excitation at 360 nm) at room temperature. The PL spectrum of the NiS nanoparticles shows a peak centered at 410 nm and 460 nm which is shorter than submicron NiS, indicating a NiS nanocrystals obtained in this work in quantum size.

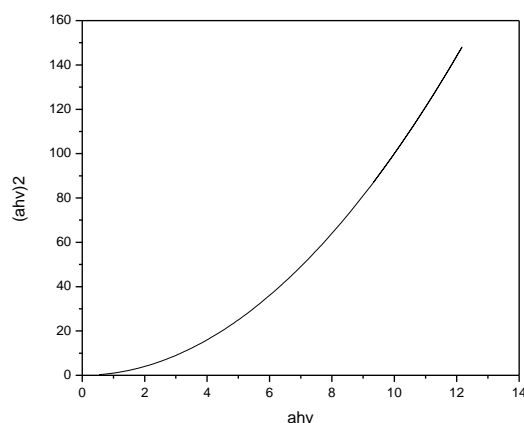


Figure 3. Graph for Energy Band Gap (U.V)

Plotting of the above graph [$ah\nu$ vs. $(ah\nu)^2$] we find that extended portion of the straight line portion of plot intersect horizontal line at 3.4 eV. So energy band gap for NiS is 3.4 eV. Where 'a' is the value of Absorption coefficient, 'h' is the value of Plank's constant is the wave number for corresponding value of wave length used in U.V. experiment.

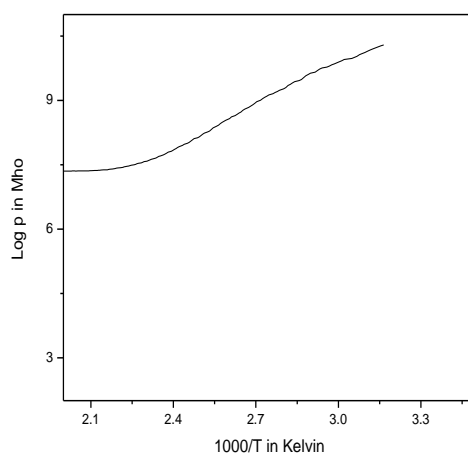


Figure 4. Graph for Resistivity vs. Temperature

Above figure gives the variation of surface resistivity of a specimen (subjected to a 2hr oxidation treatment) as a function of inverse temperature. The electrical conduction evidently is controlled by (Na^+ion) Na-4 mica shell and Ni^+ion . Hence a small polaron conduction model (Mott1968) was found to be operative in this system. In this model resistivity ρ is given by

$$\rho = \frac{KTR}{\vartheta e^2 c(1-c)} e^{(2\alpha R)} e^{(W/KT)}$$

where K is the Boltzmann constant, T the temperature the interstice separation, ϑ the optical phonon frequency, e is the electronic charge, c is the ratio of $[Ni^+]/[Ni]_{total}$, α the localization length of the localized state at the Ni ion site and W the activation energy for hopping conduction. The experimental data were least square fitted to above equation.

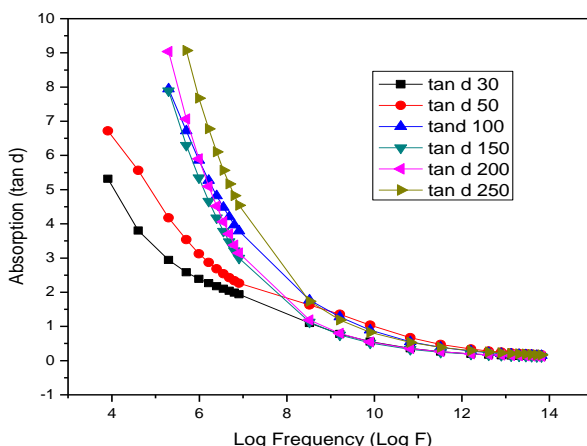


Figure 5. Graph for Absorption vs. Frequency

Dielectric properties (permittivity, loss tangent, and resistivity) of Nis Nano composites at different sintering temperature were measured within 50 Hz to 1 MHz frequency range. As shown in diagram (tan d) vs. (Log F). Relative Dielectric values for tan d do not exceed 6.74776; therefore they are within interval of .1193 to 6.74776. In the investigated frequency range, especially after curve inflection point on frequencies higher than 50 KHz, values of tan d are approximately constant, about tan d=1.094. Meanwhile, in measuring range, obtained values for ϵ_r are considerably lower in relation to well-known results, accomplished for nonlinear active dielectrics. Above fig shows frequency dependence of dielectric loss. Values of dielectric loss between .1193 to 8.973 have been obtained. The distinctly differences associated with sintering temperature can be observed in the vicinity of the inflection points. Given these absorption values, we can explicitly conclude that resonant method is not appropriate for investigation of active dielectric with such high dielectric losses. Resonant method is convenient for cases when absorption is lower than 0.05 and high Frequencies up to several hundreds of MHz. For high loss values (Loss \rightarrow 1), it is difficult to accomplish resonance and therefore attenuation occurs.

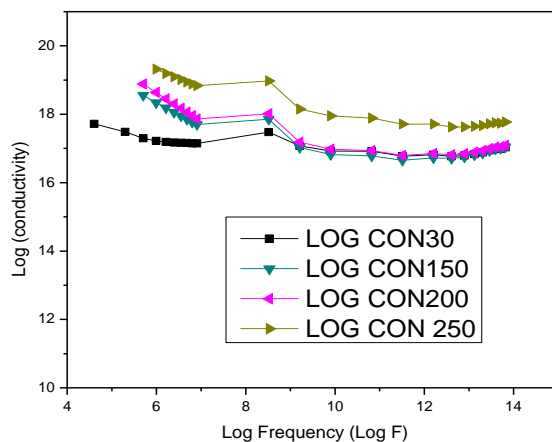


Figure 6. Graph for Conductivity vs. Frequency

It is clear that for a fixed temperature firstly conductivity increases then it shows a sharp fall and becomes saturate for a certain frequency range. The nature of curve is similar for all temperature, but values are

shifted upward as the temperature is raised. The sample exhibits conductivity with highly localized carriers bound to lattice with accompanying lattice strain i.e. with polaron conduction [2].

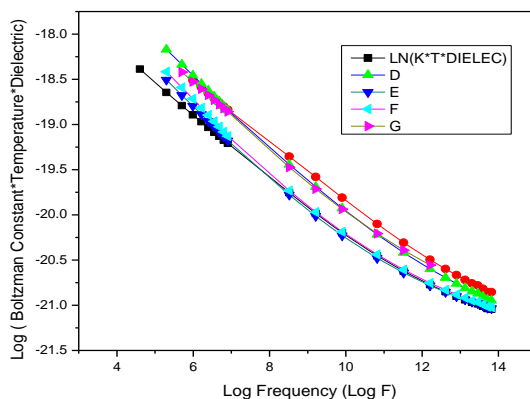


Figure 7. Graph for Calculation of Activation Energy

The a.c conductivity σ can be related to imaginary part of dielectric constant (ϵ''), $\sigma = \epsilon_0 \omega \epsilon''$. Where ϵ_0 is the permittivity of free space and ω is the angular frequency. The activation energy for conduction (E_a) in the entire region as shown in Fig. for various frequencies was calculated by fitting different regions with the equations $\sigma_{ac} = \sigma_0 e^{-E_a/k_B T}$

The ionic conductivity can be related to diffusion constant (D) using Einstein relation $\sigma/D = N/e^2 k_B T$.

This relation can be extended further as $\ln(k_B T \epsilon'') = \ln(N e^2 D_0 / \sigma_0) - \ln(\omega) - E_t / k_B T$. Where, D_0 , E_t is the maximum diffusion coefficient and total activation energy due to bulk and surface conduction, respectively. Fig shows the variation of a.c conductivity with frequency. Sharp decrease in up to 1MHz observed by Jonscher, the conductivity σ is analyzed using Jonscher power square law equation $\sigma = A \omega^s$ [3]. Where ω is angular frequency, 'A' is a constant and the exponent's 's' is a frequency-dependent parameter having values less than unity. The value of exponent 's' at different temperature is calculated by fitting the curve.

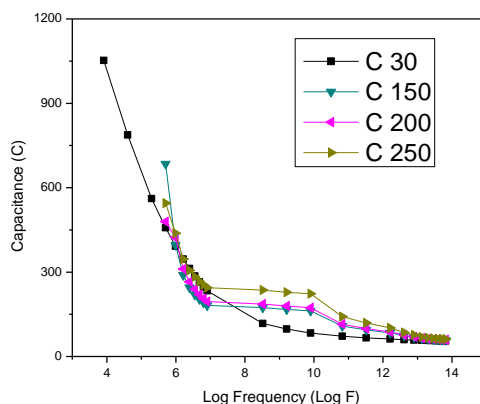


Figure 8. Graph for Capacitance vs. Log Frequency

Above graph shows a relationship between capacitance and LOG F .When we increase the temperature with increase of frequency capacitance decreases (at 30 °c and 50 °c capacitance shows a sharp fall i.e. at

higher frequency capacitance shows low value. Within a temperature range 150 °c to 250 °c capacitance also decreases with frequency but within a frequency range 1KHz to 50 KHz capacitance shows a constant value i.e. it's independent with frequency.) According to the theory capacitance of nanostructure material is primarily due to different types of polarizations present in material. Nanostructure material possesses enormous number of interfaces and the large number of defects present in these interfaces and can cause a positive and negative space charge distribution resulting in space charge polarization. The high value of capacitance at low frequencies is mainly due to space charge polarization and rotational polarization. The values are shifted upward as temperature increases (from 30 °c to 50 °c and also from 150 °c to 250 °c). As the temperature increases more and more dipole will be oriented resulting in increased value of dipole moment and also dielectric constant and capacitance of sample also. Nonuniform grains size and heterogeneous intergranular volume directly affect on dielectric and electric properties of nano crystals. This is confirmed by results for changes of permittivity, resistivity, conductivity and loss tangent. Due to such structure electron states are captured by potential barriers are named local states or extrinsic states. Within this material Electron exchange and current flow is occurred by localized electrons skip from one discrete level to another [3, 4, and 5]. This fact is exactly the reason for decreased conductivity in such type of material. Dielectric characterization implies nonhomogeneous dielectric properties in these materials. In such dielectric total current (I) resolved into two components: Active (Ia) and reactive (Ir) current. Hence for these dielectric materials each phase has proper $\tan \delta$. Consequently relaxation time also exist in such materials. Complex permittivity arises due to complex dielectric polarization. In periodic applied field and with high frequencies polarization cannot follow applied field. Hence charge flow also changes over time.

APPLICATIONS

Nickel sulfide core shell Nano rod exhibited a number of optical absorption peaks which arose because of their structural characteristics

CONCLUSIONS

The method used is simple, cheap, air stable, nontoxic, and readily available for many metal elements. This experiment process may represent a rather environmentally friendly and an approach towards many other metal sulfide nano crystals. This research may promise both adequate academic and practical interest in the development of synthetic methodologies for inorganic nano crystals and also in the field of potential applications.

REFERENCES

- [1] Mohd. Shakir, B. K. Singh, R. K. Gaur, Binay Kumar, G. Bhagavannarayana, M.A. Wahab , **2009**, 6(12), 655 – 660.
- [2] Nisha J Thayrali, R.Raveendaran, Alexandar Varghese, P.G.Vaidyan Chithra, *Indian J Eng & Mater Sci*, **2008**, 15, 489.
- [3] B.M. Tareev: Physics of Dielectric Materials, Mir Publishers, Moscow, Russia, **1979**.
- [4] M.Purenovic: Solid State Surface Reactions, SKC, NIS, Serbia, **1994**.
- [5] V.F.Korzo, V.N.Cernajeev: Dielectric Thin Films in Microelectronics, Moscow, Russia, **1977**.